*Fifth International Conference on CFD in the Process Industries*
*CSIRO, Melbourne, Australia*
*13-15 December 2006*

# COMPUTATIONAL VALIDATION AND EXTENSION OF THE GENERALISED SUTHERLAND EQUATION FOR BUBBLE-PARTICLE ENCOUNTER EFFICIENCY IN FLOTATION

**Cuong M. NGUYEN and Anh V. NGUYEN**

Chemical Engineering, The University of Newcastle, Callaghan, NSW 2308, AUSTRALIA

## ABSTRACT

Bubble-particle encounter interaction is the first step of the particle collection by rising air bubbles in flotation and has been predicted based on the potential flow condition by Sutherland and others, leading to the approximate Generalised Sutherland Equation (GSE). In this paper, the bubble-particle encounter interaction with the potential flow condition has been analysed by solving the full motion equation for the particle employing a numerical computational approach. The GSE model was compared with the numerical results for the encounter efficiency. The comparison only shows good agreement between the GSE prediction and the numerical data for very fine particles (< 15 microns in diameter), the inertial forces of which are vanishingly small. For coarser particles typically found in flotation, a significant deviation of the GSE model from the numerical data has been observed. Details of the numerical methodology and solutions for the collision angle and encounter efficiency are described in the paper. The numerical results can be used for extending the GSE theory by considering the gravitational forces and the effect of the particle density.

## NOMENCLATURE

$E$ bubble-particle encounter efficiency
$f$ drag correction factor
$g$ acceleration due to gravity
$K'$ dimensionless number, $K' = \left(1 + 0.5\delta/\rho\right)St$
$K''$ dimensionless number, $K'' = 1.5\left(\delta/\rho\right)St$
$K'''$ dimensionless number, $K''' = 2\left(\rho - \delta\right)UR_p{}^2/\left(9\mu R_b\right)$
$R$ interception number, $R = R_p/R_b$
$R_b$ bubble radius
$R_c$ radius of grazing trajectory
$R_p$ particle radius
$r$ radial coordinate (**Figure 1**)
$St$ particle Stokes number, $St = 2R_p^2U\rho/\left(9\mu R_b\right)$
$t$ time
$U$ bubble slip velocity
$v_r$ scaled particle radial velocity (divided by $U$)
$v_s$ scaled particle settling velocity (divided by $U$)
$v_\varphi$ scaled particle tangential velocity (divided by $U$)
$w_r$ scaled water radial velocity (divided by $U$)
$w_\varphi$ scaled water tangential velocity (divided by $U$)
$\beta$ dimensionless number, $\beta = 2Rf/\left(3K'''\right)$
$\delta$ water density
$\mu$ liquid viscosity
$\rho$ particle density
$\tau$ dimensionless time, $\tau = tU/R_b$
$\varphi$ polar coordinate (**Figure 1**)
$\varphi_t$ angle of tangency

## INTRODUCTION

Bubble-particle interaction is central to froth flotation widely used in the mineral industry. It is controlled by forces of various characters, including the long-range (inertial, hydrodynamic and gravitational) forces, the short-range (surface) forces, and the forces of interfacial capillarity. Since the governing forces are not interdependent, the particle-bubble interaction can conveniently be quantified by considering collision, attachment and detachment independently (Nguyen and Schulze, 2004). Collision is the approach of a particle to encounter a bubble and is governed by the fluid mechanics of the particle in the hydrodynamic force field around the bubble. The limit of the collision process is determined by the zonal boundary between the long-range hydrodynamic and interfacial force interactions (Deryaguin and Dukhin, 1960-61). The inter-surface separation distance at the zonal boundary is of the sub-micrometer order. Once the particle approaches the bubble at a shorter separation distance, the atomic, molecular and surface forces are significant and the attachment process starts. The detachment process is governed by the capillary force, the particle weight and the detaching forces due to the turbulent eddies.

The hydrodynamics of bubble-particle collision has been focused on the regime where the bubble surface is strongly retarded (immobile), caused by adsorption of surfactants, particles and other impurities from the solution (Gaudin, 1957; Flint and Howarth, 1971; Schulze, 1989; Yoon and Luttrell, 1989; Finch and Dobby, 1990; Nguyen, 1994). In recent years bubble-particle collision with a mobile bubble surface has attracted intensive research (Dai et al., 1998; Dai et al., 2000). Research into the collision of bubbles with a mobile surface is driven by the fact that various surface contaminants on a bubble surface are in a dynamic state, known as a dynamic adsorption layer, and that during bubble rise in a flotation cell the surface contaminants are swept to the rear surface of the bubble by adjacent water. Thus, the forward part of bubble surfaces can remain mobile even when the bubbles reach terminal velocity, i.e. even when equilibrium of the mass transfer of surfactants is established. While the forward surface of bubbles in solutions is mobile, the surface contamination often forms an immobile (stagnant) cap at the rear (Clift et al., 1978; Sam et al., 1996; Zhang and Finch, 2001). It now can be established that not only

the surface of fresh bubbles is mobile, but the forward surface of aged bubbles on which bubble-particle interaction in actual flotation takes place can also be mobile. At the mobile surface of air bubbles, the tangential component of the liquid velocity is non-zero, but the condition of zero tangential stress is applied. At the immobile surface, both of the velocity component and stress are zero.

The first model of bubble-particle interaction with a mobile bubble surface was published by K. L. Sutherland from CSIRO Minerals (Sutherland, 1948), who assumed water in a flotation cell to be described by the potential flow and employed a simplified particle motion equation without inertia. The Sutherland prediction for the bubble-particle encounter efficiency, *E*, is described by $E = 3R$, where *R* is the interception number, defined as the ratio of the particle to bubble radius, $R = R_p / R_b$. The Sutherland model was found to over-predict the encounter efficiency and has been improved by incorporating inertial forces which are magnified at the mobile surface with a non-zero tangential velocity component of the liquid phase. For example, the Sutherland equation was extended to account for the influence of the inertial forces by Dukhin (Dukhin, 1983). Nowadays, this extension, referred to as the Generalised Sutherland Equation (GSE), is described by (Dai et al., 1998):

$$E = 3R\ \sin^2\varphi_t \exp\left\{-\cos\varphi_t\left[3K'''\left(\ln R + 1.8\right) + \left(8 - 12\cos\varphi_t + 4\cos^3\varphi_t\right)/\left(3\sin^4\varphi_t\right)\right]\right\} \quad (1)$$

where the angle of tangency, $\varphi_t$, is described as

$$\varphi_t = \arccos\left(\sqrt{1+\beta^2} - \beta\right) \quad (2)$$

Parameters $\beta$ and $K'''$ in these equations are defined by

$$K''' = \frac{2\left(\rho - \delta\right)UR_p^{\ 2}}{9\mu R_b} \quad (3)$$

$$\beta = \frac{2Rf}{3K'''} \quad (4)$$

where *U* is the bubble (slip) velocity relative to the liquid phase, $\rho$ and $\delta$ are the particle and liquid densities, $\mu$ is the liquid viscosity. The drag correction, *f*, in Eq. (4) was not considered by Dukhin (Dukhin, 1983) (*f* = 1), but it was later changed to *f* = 2 (Dai et al., 1998).

In this paper, the (analytical) Generalised Sutherland Equation will be validated and extended using the exact computational solutions of the particle motion equation employed in the Sutherland theory.

## COMPUTATIONAL VALIDATION OF THE GSE

The bubble-particle encounter interaction in flotation is schematically shown in **Figure 1**. The following equation for particle motion was used to obtain Eq. (1) for the Generalised Sutherland Equation (Dukhin, 1983; Dai et al., 1998):

$$K'\frac{d\vec{v}}{d\tau} - K''\frac{d\vec{w}}{d\tau} = \vec{w} - \vec{v} \quad (5)$$

where *v* and *w* describe the dimensionless particle and water velocities around the bubble surface, and the arrows over the symbols are used to describe the vectors. The dimensionless velocities are obtained by dividing the appropriate dimensional velocities by the bubble slip velocity, *U*. The dimensionless time in Eq. (5) is defined as $\tau = tU / R_b$, where *t* is the dimensional time. The dimensionless numbers describing the inertial effects are defined as $K' = \left(1 + 0.5\delta/\rho\right)St$ and $K'' = 1.5\left(\delta/\rho\right)St$, where the particle Stokes number is defined as $St = 2R_p^2 U\rho/\left(9\mu R_b\right)$.

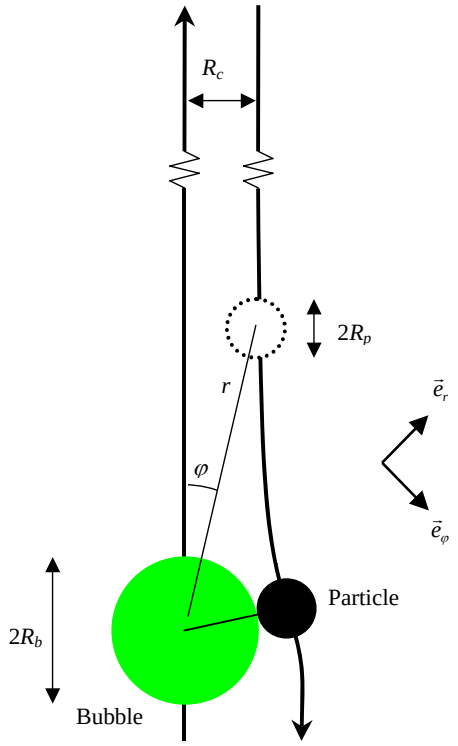


**Figure 1**: Schematic of the bubble-particle encounter interaction. The collision radius, $R_c$, is measured by the distance between the parallel lines of the path of the rising bubble and the grazing trajectory of settling particles when being far apart from the bubble surface. $\vec{e}_r$ and $\vec{e}_\varphi$ describe the unit vectors of the rotationally symmetrical coordinate system $\left(r, \varphi\right)$.

Equation (5) can be further simplified by considering the steady flow of the liquid, $\partial\vec{w}/\partial\tau = 0$ and the rotational symmetry of the bubble-particle interaction, giving

$$K'\frac{dv_r}{d\tau} = K'\frac{v_\varphi^{\ 2}}{r} + K''\left(w_r\frac{\partial w_r}{\partial r} + \frac{w_\varphi}{r}\frac{\partial w_r}{\partial \varphi} - \frac{w_\varphi^{\ 2}}{r}\right) + w_r - v_r \quad (6)$$

$$K'\frac{dv_r}{d\tau} = -K'\frac{v_\varphi v_r}{r} + K''\left(w_r\frac{\partial w_\varphi}{\partial r} + \frac{w_\varphi}{r}\frac{\partial w_\varphi}{\partial \varphi} + \frac{w_\varphi w_r}{r}\right) + w_\varphi - v_\varphi \quad (7)$$

where $v_r$ and $v_\varphi$ are the radial and tangential components of the particle velocity, which are functions of the particle radial, $r$, and polar, $\varphi$, positions and can be described as

$$v_r = \frac{dr}{d\tau} \tag{8}$$

$$v_\varphi = r\frac{d\varphi}{d\tau} \tag{9}$$

The liquid velocity components contained in the above motion equation can be determined from the potential flow used in deriving the Generalised Sutherland Equation (Dukhin, 1983; Dai et al., 1998), giving $w_r = -\left(1-r^{-3}\right)\cos\varphi$ and $w_\varphi = \left(1+0.5r^{-3}\right)\sin\varphi$. The initial conditions for the differential equations for particle motion are described as $v_r\left(r=\infty\right) = -\cos\varphi$ and $v_\varphi\left(r=\infty\right) = \sin\varphi$.

The particle motion Eqs. (6) and (7) were approximately solved to obtain the analytical solution for the GSE described by Eq. (1) (Dukhin, 1983; Dai et al., 1998). To validate the GSE theory, Eqs. (6) and (7) are numerically solved using the fourth-order Runge-Kutta method. The initial position $\left(r_0, \varphi_0\right)$ of the particle position needed for the numerical integration using the fourth-order Runge-Kutta method can be chosen but it has to be sufficient far from the bubble surface, where the initial condition at infinity is satisfied. The particle trajectories far from the bubble surface are not influenced by the bubble surface and should be parallel. Eqs. (6) - (9) were discretised following the standard procedure of the Runge-Kutte method for a system of differential equations of the first order (Rice and Do, 1995).

The grazing trajectory for particle motion can be computationally found using the condition that there exists only one contact point between the bubble surface and the particle on the grazing trajectory. In this paper, this condition was computationally satisfied by trial-and-error, varying the initial particle position $\left(r_0, \varphi_0\right)$. A particle position very close to the symmetric axis of the bubble rise was initially chosen to start the numerical integration for obtaining a particle trajectory. If the trajectory reached a point away from the bubble surface by[†] $\left(1+R\right)$, the integration was stopped and the initially chosen particle position was shifted away from the axis of symmetry by a very small increment, which was typically about $1\times10^{-3}$. The new particle position was then used to calculate the corresponding trajectory for the particle. The contact between the bubble and particle surfaces was checked and the computation procedure was repeated until no contact was found computationally. The last trajectory was considered as the grazing trajectory. The polar position of the bubble-particle contact obtained with the last trajectory was determined to give the angle of tangency, $\varphi_t$. The distance between the parallel part of the last trajectory and the axis of symmetry was determined to give the collision radius, $R_c$, as shown in **Figure 1**. The encounter efficiency was calculated using the following equation:

$$E = \left\{\frac{R_c}{R_b + R_p}\right\}^2 \tag{10}$$

The error in the computational determination of the encounter efficiency was found to be about $\pm1\times10^{-6}$.

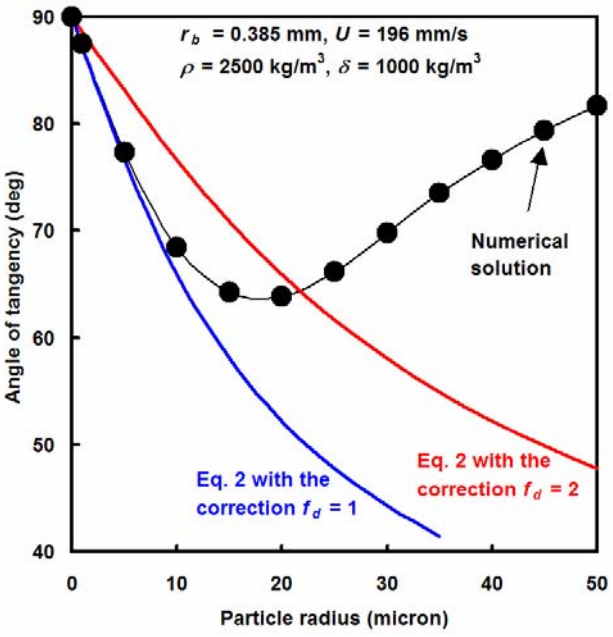


**Figure 2**: Comparison between the computational results and Eq. (2) with $f_d$ = 1 (Dukhin, 1983) and $f_d$ = 2 (Dai et al., 1998) for the angle of tangency, $\varphi_t$, versus the particle (quartz) radius.

Comparison between the computational solutions and analytical solutions for the angle of tangency, $\varphi_t$, described by Eq. (2) is shown in **Figure 2**. Good agreement between the computational results and the analytical solutions is observed only for (ultrafine) particles with radius smaller than 5 microns. **Figure 2** shows significant deviation of the analytical solutions for particles with radius bigger than 20 microns. Importantly, all the analytical solutions predict that the angle of tangency decreases with increasing particle radius, while the exact numerical solutions only show the decrease for very small (ultrafine) particles. There exists a particle size where the angle of tangency has a minimum. Beyond this minimum, other inertial effects are greater than the centrifugal effect, leading to the increase in the angle of tangency towards 90 degrees when the inertial effects control the bubble-particle encounter and collision. Because Eq. (2) has been used for predicting the attachment efficiency (Dai et al., 1999; Ralston et al., 2002; Duan et al., 2003; Pyke et al., 2003), the significant difference in the angle of tangency shown in **Figure 2** will have a significant consequence in the modeling and predicting bubble-particle attachment interaction in flotation, in particular in flotation of non-ultrafine particles.

[†] Note that the dimensionless radial coordinate for the centre of particle in contact with the bubble surface is $\left(R_b + R_p\right)/R_b = 1+R$.

Comparisons between the computational solution and the GSE Eq. (1) and Sutherland original equation for the encounter efficiency are shown in **Figure 3**. Good agreement between the GSE equation and the computational results is only observed for ultrafine particles. The deviation of the GSE equation from the computational results is significant for non-ultrafine particles. Interestingly, the prediction by the original Sutherland equation is closer to the computational results for non-ultrafine particles.

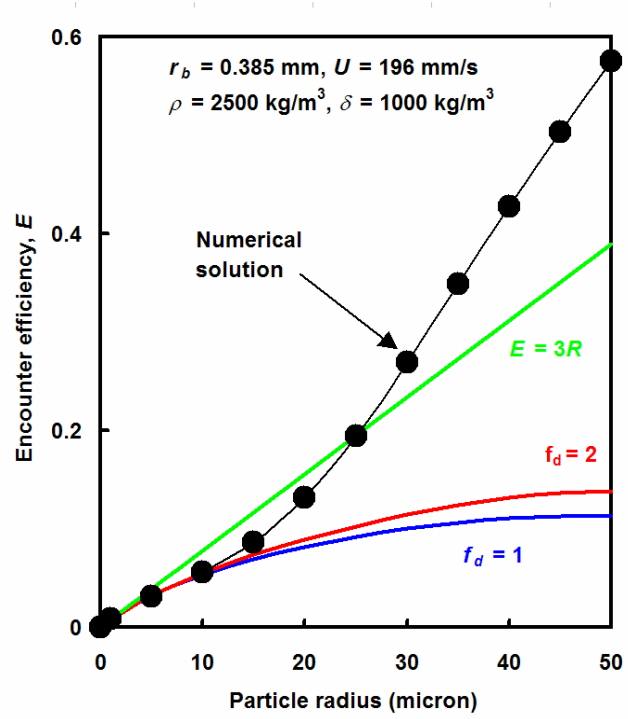


**Figure 3**: Comparison between the computational results (points) and the Sutherland Equation, $E= 3R$, and Generalised Sutherland Equation (Dai et al., 1998; Ralston et al., 1999), i.e. Eq. (1) with $f_d$ = 1 or 2, for the encounter efficiency, $E$, versus the particle (quartz) radius.

## COMPUTATIONAL EXTENSION OF THE GSE

The key equation of the GSE theory is described by Eq. (5) which does not contain gravitational forces. The first extension of the GSE theory is to include the particle weight and buoyancy. The extended equations useful for the numerical integration can be obtained from Eqs. (6) and (7), giving

$$K'\frac{dv_r}{d\tau} = K'\frac{v_\varphi^{\,2}}{r} + K''\left( w_r\frac{\partial w_r}{\partial r} + \frac{w_\varphi}{r}\frac{\partial w_r}{\partial \varphi} - \frac{w_\varphi^{\,2}}{r}\right) + w_r - v_r - v_s\cos\varphi \qquad (11)$$

$$K'\frac{dv_r}{d\tau} = -K'\frac{v_\varphi v_r}{r} + K''\left( w_r\frac{\partial w_\varphi}{\partial r} + \frac{w_\varphi}{r}\frac{\partial w_\varphi}{\partial \varphi} + \frac{w_\varphi w_r}{r}\right) + w_\varphi - v_\varphi + v_s\sin\varphi \qquad (12)$$

where $v_s$ accounts for the effect of the gravitation forces on the bubble-particle encounter interaction and is described as

$$v_s = \frac{2R_p^2(\rho-\delta)g}{9\mu U} \qquad (13)$$

Equations (11) and (12) can numerically be integrated following the same technique and procedure described in the previous section. The angle of tangency and the encounter efficiency can be determined similarly.

The numerical results are shown in **Figure 4** and **Figure 5** for the angle of tangency and encounter efficiency, respectively. The particle density has very strong effect on the angle of tangency and encounter efficiency. The deviation of the angle of tangency from 90 degrees is significant at low density. Similarly to the results presented in the previous section, the angle of tangency decreases from 90 degrees with increasing the particle size, reaching a minimum and then creasing back to 90 degrees. This feature of our computational modelling is beyond the capability of the generalised Sutherland theory.

The influence of the particle density on the encounter efficiency is significant for coarse particles as can be seen from **Figure 5**. Again, the feature is beyond the scope of the generalised Sutherland theory. Finally, the efficiency increases with increasing the particle density and size as expected.

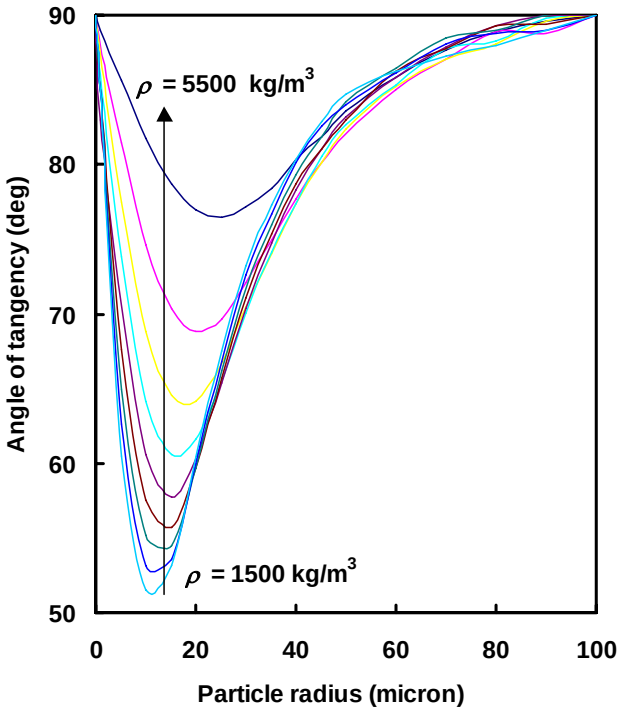


**Figure 4**: Numerical results for the angle of tangency versus the particle size and density as obtained from Eqs. (11) and (12) for the extended generalised Sutherland theory. The bubble size and rise velocity are the same as those shown in **Figure 2**. The particle density increment is 500 kg/m$^3$.

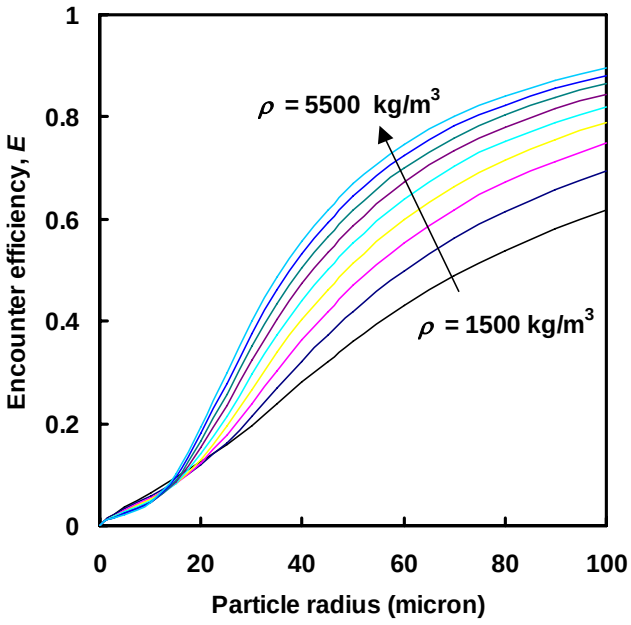


**Figure 5**: Numerical results for the encounter efficiency versus the particle size and density as obtained from Eqs. (11) and (12) for the extended generalised Sutherland theory. The bubble size and rise velocity are the same as those shown in **Figure 2**. The particle density increment is 500 kg/m$^3$.

## CONCLUSION

The particle encounter interaction with an air bubble with a mobile surface has been computationally analyzed. The computational results have been used to validate Sutherland's theory on the bubble-particle collision interaction and its generalization with the inclusion of the centrifugal (inertial) effect. It was shown in the paper that the generalised Sutherland theory only agreed with the computational simulation for very fine particles (< 10 microns in diameter). For non-ultrafine particles, a significant deviation of the GSE model from the numerical data has been observed for the angle of tangency and the encounter efficiency. The computational modelling has been extended to include gravitational forces. The extended generalised theory shows very significant effect of the particle density on the angle of tangency as well as on the encounter efficiency. Finally, the computational results show that there exists a particle size where the angle of tangency has a minimum. For bigger particles, the other inertial effects on particle collision are more significant than the centrifugal effect and, consequently, the angle of tangency increases with increasing particle size towards 90 degrees. The deviation of the angle of tangency shown in this paper will have a significant consequence in modeling and predicting the particle attachment by air bubbles in flotation.

## ACKNOWLEDGEMENT

The authors acknowledge the Australia Research Council for financial support through an International Linkage grant.

## REFERENCES

CLIFT, R. et al., (1978), "Bubbles, Drops and Particles". Academic Press, New York, 380 pp.

DAI, Z. et al., (1998), "The inertial hydrodynamic interaction of particles and rising bubbles with mobile surfaces", *J. Colloid Interface Sci.*, **197,** 275-292.

DAI, Z. et al., (1999), "Particle-bubble attachment in mineral flotation", *J. Colloid Interface Sci.*, **217,** 70-76.

DAI, Z. et al., (2000), "Particle-bubble collision models - a review", *Adv. Colloid Interface Sci.*, **85,** 231-256.

DERYAGUIN, B.V. and DUKHIN, S.S., (1960-61), "Theory of flotation of small and medium size particles", *Trans. Inst. Min. Metall.*, **70,** 221-233.

DUAN, J. et al., (2003), "Calculation of the flotation rate constant of chalcopyrite particles in an ore", *International Journal of Mineral Processing*, **72,** 227-237.

DUKHIN, S.S., (1983), "Critical value of the Stokes number and the Sutherland formula", *Kolloidn. Zh.*, **45,** 207-18.

FINCH, J.A. and DOBBY, G.S., (1990), "Column Flotation". Pergamon, Oxford, 180 pp.

FLINT, L.R. and HOWARTH, W.J., (1971), "Collision efficiency of small particles with spherical air bubbles", *Chem. Eng. Sci.*, **26,** 1155-68.

GAUDIN, A.M., (1957), "Flotation". McGraw-Hill, New York.

NGUYEN, A.V., (1994), "The collision between fine particles and single air bubbles in flotation", *J. Colloid Interface Sci.*, **162,** 123-8.

NGUYEN, A.V. and SCHULZE, H.J., (2004), "Colloidal science of flotation". Marcel Dekker, New York, 840 pp.

PYKE, B. et al., (2003), "Bubble particle heterocoagulation under turbulent conditions", *Journal of Colloid and Interface Science*, **265,** 141-151.

RALSTON, J. et al., (1999), "Inertial hydrodynamic particle-bubble interaction in flotation", *Int. J. Miner. Process.*, **56,** 207-256.

RALSTON, J. et al., (2002), "Wetting film stability and flotation kinetics", *Advances in Colloid and Interface Science*, **95,** 145-236.

RICE, R.G. and DO, D.D., (1995), "Applied Mathematics and Modelling for Chemical Engineers". John Willey & Sons, New York, NY, 706 pp.

SAM, A. et al., (1996), "Axial velocity profiles of single bubbles in water/frother solutions", *Int. J. Miner. Process.*, **47,** 177-196.

SCHULZE, H.J., (1989), "Hydrodynamics of bubble-mineral particle collisions", *Miner. Process. Extract. Met. Rev.*, **5,** 43-76.

SUTHERLAND, K., (1948), "The physical chemistry of flotation XI. Kinetics of the flotation process", *J. Phys. Chem.*, **52,** 394-425.

YOON, R.H. and LUTTRELL, G.H., (1989), "The effect of bubble size on fine particle flotation", *Miner. Proc. Extract. Met. Rev.*, **5,** 101-122.

ZHANG, Y. and FINCH, J.A., (2001), "A note on single bubble motion in surfactant solutions", *Journal of Fluid Mechanics*, **429,** 63-66.